Bioengineering **2014**, *1*, 85-110; doi:10.3390/bioengineering1010085

OPEN ACCESS

bioengineering

ISSN 2306-5354

www.mdpi.com/journal/bioengineering

Article

Biofabrication Using Pyrrole Electropolymerization for the Immobilization of Glucose Oxidase and Lactate Oxidase on Implanted Microfabricated Biotransducers

Christian N. Kotanen [1,2], Olukayode Karunwi [1,2] and Anthony Guiseppi-Elie [1,2,3,4,5,*]

[1] Center for Bioelectronics, Biosensors and Biochips (C3B), Clemson University Advanced Materials Center, Anderson, SC 29625, USA; E-Mails: ckotane@clemson.edu (C.N.K.); okarunw@clemson.edu (O.K.)

[2] Department of Bioengineering, College of Engineering and Science, Clemson University, 301 Rhodes Research Center, Clemson, SC 29634, USA

[3] Department of Chemical and Biomolecular Engineering, College of Engineering and Science, Clemson University, 132 Earle Hall, Clemson, SC 29634, USA

[4] Holcombe Department of Electrical and Computer Engineering, College of Engineering and Science, Clemson University, 105 Riggs Hall, Clemson, SC 29634, USA

[5] ABTECH Scientific, Inc., Biotechnology Research Park, 800 East Leigh Street, Richmond, VA 23219, USA

***** Author to whom correspondence should be addressed; E-Mail: guiseppi@clemson.edu; Tel.: +1-864-656-1712; Fax: +1-864-656-1713.

Received: 26 December 2013; in revised form: 1 March 2014 / Accepted: 12 March 2014 / Published: 18 March 2014

Abstract: The dual responsive Electrochemical Cell-on-a-Chip Microdisc Electrode Array (ECC MDEA 5037) is a recently developed electrochemical transducer for use in a wireless, implantable biosensor system for the continuous measurement of interstitial glucose and lactate. Fabrication of the biorecognition membrane via pyrrole electropolymerization and both *in vitro* and *in vivo* characterization of the resulting biotransducer is described. The influence of EDC-NHS covalent conjugation of glucose oxidase with 4-(3-pyrrolyl) butyric acid (monomerization) and with 4-sulfobenzoic acid (sulfonization) on biosensor performance was examined. As the extent of enzyme conjugation was increased sensitivity decreased for monomerized enzymes but increased for sulfonized enzymes. Implanted biotransducers were examined in a Sprague-Dawley rat hemorrhage model. Resection after 4 h and subsequent *in vitro* re-characterization showed a decreased sensitivity from

0.68 (±0.40) to 0.22 (±0.17) $\mu A \cdot cm^{-2} \cdot mM^{-1}$, an increase in the limit of detection from 0.05 (±0.03) to 0.27 (±0.27) mM and a six-fold increase in the response time from 41 (±18) to 244 (±193) s. This evidence reconfirms the importance of biofouling at the bio-abio interface and the need for mitigation strategies to address the foreign body response.

Keywords: biofabrication; pyrrole; polypyrrole; electropolymerization; biosensors; amperometry; glucose oxidase; glucose; *in vivo*; hemorrhage

1. Introduction

The fabrication of multi-analyte biotransducers is a major technical challenge when the length scales of the individual transducer elements are on the order of microns [1–3]. Such biotransducers are critical for *in vivo* (intramuscular) wireless biosensor systems [4] that allow for immediate and continual pre-hospital monitoring of lactate and glucose to inform patient specific interventions that will improve survivability from hemorrhage [2,4]. Continued examination of interstitial compartments using biosensors will aid in understanding the temporal relationships among biomarkers of stress in these environments and how they relate to hemorrhagic shock states [5]. Electropolymerization of conductive polymers such as polypyrrole [6–8] and polyaniline [9,10], as well as electropolymerization of non-conductive polymers, such as poly(*o*-phenylenediamine) [11], poly(*m*-phenylenediamine) [12,13] and poly(phenylene oxide) [14,15], have been well studied and is one of the emerging additive methods of biofabrication that may be used to guide and deposit biological entities such as enzymes, antibodies, nucleic acids, sub-cellular fragments, and even whole cells to metallic or semi-conducting electrode sites of more complex devices [16–18]. Biofabrication techniques using conducting electroactive polymers have been previously described for use in the design and fabrication of the biological recognition membranes of biotransducers [17,19]. Polypyrrole is a conductive electroactive polymer electropolymerized from its monomer pyrrole, which, because of its facility to direct the deposition of dopant and entrained macromolecules onto electrode surfaces, has been previously described and reviewed for the fabrication of amperometric, voltammetric, and impedimetric biotransducers [20–22].

Biorecognition membranes of precisely controlled thickness may be fabricated through judicious control of electropolymerization charge density [23]. In so doing, a wide range of copolymers may be synthesized and a wide range of monomeric and polymeric dopants may be incorporated through judicious control of the materials and solvent composition of the electropolymerization bath [24,25]. In addition, post-processing of biorecognition membrane layers, such as over oxidation or chemical derivatization may be used to enhance or stabilize performance of the fabricated bio-layer. Most importantly, all these processing steps may be performed in batch or continuous mode, in bio-benign aqueous environments at pH values close to 7.0 and with the use of modest electrode potentials under conditions that are close to ambient; conditions that are compatible with biological recognition entities and that prevent denaturation. Thus, conducting electroactive polymers (CEPs) have many attractive features such as selectivity of enzyme entrapment to electrode surfaces [26,27], reduction of interfacial impedance, thickness control via charge density [28], enzyme stability, biocompatibility [29–31], and adjustment of biosensor enzyme kinetic properties. Polypyrrole, along with other electroactive polymers,

once formed, can be surface modified and used for various chemical coupling reactions [32,33]. During electropolymerization, the biological molecule may serve as the dopant anion (most enzymes possess a net negative charge). Hence, biomolecules, such as enzymes, can be used to dope polypyrrole during electropolymerization when fabricating biosensors [17,27,34,35]. Enzymes such as glucose oxidase possess amino acid residues in their primary structure to which covalent coupling of other functional moieties can be performed. For instance GOx from *Aspergillus niger* (EC 1.1.3.4, PDB ID 1CF3) has 15 lysine residues per subunit (two subunits per molecule of GOx) possessing primary amines available for covalent chemical modification. The covalent chemical modification of an enzyme in such a manner has the potential to influence the extent of its incorporation into the biorecognition membrane layer during the electropolymerization process.

Biotransducers fabricated with electroconductive hydrogels (ECHs) [35,36] offer the tremendous benefits of enzyme stability and protection from proteases in the host environment during *in vivo* application [35] but with a drawback of suboptimal sensitivity and compromised limits of detection for a wireless biosensor system [2,35]. It is believed that enzyme loading (Units/cm^2) and transport limitations compromise performance. Through enzyme modification that aims to improve incorporation (loading), it should be possible to enhance current densities of polypyrrole-based amperometric biosensors. As a direct means of improving biosensor performance, *i.e.*, increasing biosensor sensitivity and maximum current, lysine groups of enzymes were functionalized with (i) a pyrrole moiety (monomerization) thereby directly incorporating enzymes via co-polymerization into the growing polypyrrole layer, or (ii) a sulfonic acid moiety (sulfonization) thereby incorporating enzymes as better dopants into the growing polypyrrole layer. Both non-covalent and covalent enzyme modifications via monomerization and sulfonization were performed and the influence of these on biosensor performance was studied. Furthermore, the effect of a polypyrrole-polystyrenesulfonate (PPy-PSSA) seeding layer of low charge density (10 mC/cm^2) intended to create a "flash" of highly adherent but otherwise porous PPy on the electrodes was developed as a means to enhance biofabrication and bioanalytical performance of subsequent enzyme layers.

The *in vivo* performance of a biosensor system [37], based on the MDEA 5037 fabricated with electropolymerized polypyrrole, was examined in a Sprague-Dawley animal model. Previous characterizations of these systems *in vitro* have been performed and performance parameters of sensitivity, apparent Michaelis-Menten constant, limits of detection, stability, biosensor channel crosstalk, and linear range have been examined [2,27,35,38]. Sensors fabricated with polypyrrole-based electroconductive hydrogels have shown no loss of sensitivity *in vitro* over an 18-day period when stored in PBS buffer at 4 ℃ [38]. Glucose biosensors fabricated with overoxidized polypyrrole were observed to limit the response to ascorbic acid to no more than 5% of the total response to glucose, reduce signal response to other negatively charged endogenous interferents by 92% and have an interferent rejection ratio of 12:1 [35,38]. Nonspecific adsorption of enzymes companion sites during the biofabrication process has been shown to be insignificant and to have little to no influence on biosensor response [2]. Dual analyte electrochemical biotransducers for the amperometric detection of glucose and lactate have been developed for use in thin layer flow cells that employ flow injection analysis [39]. The current transducers, developed in conjunction with ABTECH Scientific, Inc. (Richmond, VA, USA), were microlithographically fabricated, decorated with the biorecognition layer, characterized *in vitro*, and implanted into the trapezius muscle of Sprague Dawley rats. Internal

calibration, response under controlled hemorrhage conditions, and post–resection re-characterization were used to evaluate biotransducer performance.

2. Experimental Section

2.1. Chemicals and Reagents

Poly(styrene sulfonic acid) (PSSA 30%, MW = 70,000, 6–10% sulfonation, ρ = 1.10 g/mL) was purchased from Polysciences, Inc. Dulbecco's phosphate buffered saline, benzophenone (reagent grade 99%), pyrrole monomer (reagent grade 98+%), 4-(3-pyrrolyl)butyric acid (PyBA), glucose oxidase (GOx, E.C. 1.1.3.4 from *Aspergillus niger*), β-D(+)-glucose, 1-ethyl-3-[3-dimethylaminopropyl] carbodiimide (EDC), *N*-hydroxysulfosuccinimide (Sulfo-NHS), N-hydroxysuccinimide (NHS), 4-sulfobenzoic acid (SBA), ferrocene monocarboxylic acid (FcCOOH), and all other common solvents, were purchased from Sigma Aldrich Co. (St. Louis, MO, USA). Pyrrole monomer was purified by double passage through an alumina silicate column (Supelclean™, LC-Alumina-A SPE, 570*2-U, 1 g). Solutions were prepared in deionized water (DI-water) prepared by purifying distilled water through a Milli-Q® plus (Millipore Inc.) ultrapure water system. The glucose stock solution of 1.0 M was prepared and allowed to mutarotate overnight before use. Phosphate buffered saline (PBS) was used at 0.1 M at pH = 7.2 unless noted otherwise.

2.2. Enzyme Monomerization and Sulfonization

4-(3-pyrrolyl)butyric acid (for monomerization) and 4-sulfobenzoic acid (for sulfonization/ dopantization) were covalently conjugated to amine groups of lysine residues of glucose oxidase. For monomerization of enzymes, a solution of 0.175 M Py and 0.025 M PyBA was prepared in DI-water and its pH adjusted to 4.5–5.5 using dropwise addition of 1.0 M NaOH. For sulfonization of enzymes, a solution of 0.2 M Py and 0.625 mM SBA was prepared in DI-water (pH ≈ 4–4.5 without need for adjustment). The acid groups of PyBA or SBA were activated by the addition of 0.625 mM EDC, the concentration needed to achieve a 10:1 mole ratio of PyBA:GOx or SBA:GOx, was incorporated and allowed to incubate for 1 h at 25 °C. Next 0.625 mM of NHS was incorporated and the solution allowed to incubate for 5 min at 25 °C. Finally, 1.0 mg/mL of GOx was incorporated, the solution shaken vigorously and allowed to incubate for 24 h at 4 °C. This process was repeated to achieve a 2:1 mole ratio of PyBA:GOx or SBA:GOx in conjugation and was repeated without EDC-NHS coupling to serve as the non-conjugated controls.

2.3. Electropolymerization and Electrochemical Characterization

Electropolymerization of pyrrole and electrochemical characterization of polypyrrole thin films were performed using a PAR 283 Potentiostat/Galvanostat (Princeton Applied Research) equipped with PowerSuite® software and a BAS-100B/W Electrochemical Analyzer with a BAS PA-1 preamplifier module used to amplify the current and to filter out noise (BASi, West Lafayette, IN, USA). All experiments were carried out in a three-electrode setup with platinum microelectrodes (ϕ = 100 μm; BASi), the Electrochemical Cell-on-a-Chip Microdisc Electrode Arrays (ECC MDEA

5037-Pt; ABTECH Scientific, Inc.) as the working electrode, an Ag/AgCl (3 M KCl) reference electrode (RE803; ABTECH Scientific, Inc.) and a large area platinum mesh counter electrode.

2.4. Transducer Cleaning and Seeding with Polypyrrole

Two types of electrochemical transducers were used; platinum microelectrodes (μE) for the *in vitro* characterization of polymer films and microlithographically fabricated micro disc electrode arrays (MDEA) for animal implantation. The platinum microelectrode was mechanically polished for 1 min using 1.0 μm diamond slurry and then washed with methanol. This was followed by further polishing for 1 min using 0.05 μm alumina and rinsed with DI-water in order to expose a fresh platinum surface. Electrodes were subsequently ultrasonicated, for 3 min each in DI-water, propanol, DI-water; cleaned in a UV-ozone Cleaner (Boekel Industries, Philadelphia, PA, USA) and cathodically cleaned by repeated cycling over the range 0.0 to −1.2 V in phosphate buffered saline (PBS) *vs.* Ag/AgCl [40]. The ECC MDEA 5037-Pt is a microlithographically fabricated dual analyte electrochemical transducer intended for amperometric and voltammetric biosensor application. Developed for simultaneous monitoring of interstitial glucose and lactate [1]. The transducer possesses 37 recessed microdiscs arranged in a hexagonal array. Each disc has φ = 50 microns for a total working electrode area, WEA = 7.3×10^{-4} cm^2 [41]. The microlithographic fabrication and geometric patterning of the three-electrode electrochemical biotransducers have been previously described [41] and assembly and packaging of the chip in a manner suitable for implantation into small vertebrate animals has similarly been described [42]. In summary, the electrochemical transducers (0.2 cm × 0.4 cm × 0.05 cm) were fabricated from electron beam vapor deposited platinum (100 nm) on an adhesion promoting titanium/tungsten (Ti/W) layer (10 nm) onto a 0.5 mm thick electronics grade borosilicate glass (Schott D263). The electrodes were laid out as two separate three-electrode electrochemical cells and the metallization passivated with 0.5 micron thick silicon nitride (Si_3N_4). The nitride layer was eventually patterned and fluoro-plasma etched to reveal the array of multiple microdiscs of the working electrode (7.3×10^{-4} cm^2) the large area counter electrode (7.3×10^{-3} cm^2) and the shared reference electrode (7.3×10^{-5} cm^2) that were connected to the five bonding pads. The MDEA 5037-Pt transducer was first ultrasonicated for 3 min in each of DI-water, isopropyl alcohol (IPA), and DI-water. Next, the transducer was placed in a UV-ozone cleaner (Boekel Industries) under irradiated ozone generation for 10 min followed by 1 min of ultrasonication in IPA. This was followed by plasma surface modification of the transducer to generate hydroxyl groups on the silicon nitride surface (Harrick Plasma Cleaner). The transducer was then immersed in PBS buffer, made the working electrode of a three electrode electrochemical cell and was cathodically cleaned by sweeping the potential between 0 to −1.2 V *vs.* Ag/AgCl at 100 mV/s for 40 cycles.

In general, biospecificity was conferred to each array-working electrode of the device by immobilizing a bioreceptor to each working electrode. To support robust biorecognition membrane formation, electrodes were first seeded with a thin electropolymerized film of PSSA doped polypyrrole (PPy-PSSA). This adherent film was formed via potentiostatic electrosynthesis at 750 mV *vs.* Ag/AgCl to a charge density of 10 mC/cm^2 from an aqueous solution of 0.2 M Py and 0.05 M repeat units of PSSA as dopant prepared in DI-water and pH-adjusted to pH = 4.75 using 0.1 M NaOH [21,35].

2.5. Conferring Biospecificity to Polypyrrole Seeded Transducers

Following covalent or non-covalent conjugation, biospecificity was conferred to the microelectrodes through further electropolymerization in the freshly prepared conjugation solutions to form the covalently conjugated polypyrrole systems of PPy(SBA-*con*-GOx) and P(Py-*co*-PyBA-*con*-GOx). Non-covalently conjugated systems, useful as controls, did not incorporate EDC or NHS in the electropolymerization reaction solutions and these resulted in the following systems of PPy(SBA)-GOx, P(Py-*co*-PyBA)-GOx. Further control systems (PPy-GOx) were prepared with 0.2 M Py and 1 mg/mL GOx in DI-Water. After preparation, biotransducers were placed in PBS and refrigerated at 4 ℃ over night to allow for non-specifically adsorbed enzymes to leach out. Biospecificity was then conferred to the working electrode arrays through further electropolymerization in solutions containing 0.175 M Py, 0.025 M PyBA, and 1 mg/mL of GOx or LOx prepared in DI-Water with pH adjustment to 4.5–5.5 using 1 M NaOH. Electropolymerization for entrapping enzymes proceeded at 850 mV *vs.* Ag/AgCl for 100 mC/cm^2. Before use, enzyme-modified microelectrodes were over-oxidized (OO-PPy) by repeatedly cycling the electrode in PBKCl (100 mM, pH 7.2) between −200 to 1,300 mV *vs.* Ag/AgCl for 40 cycles.

2.6. In Vitro Biosensor Calibration Prior to in Vivo Implantation

The 8100-K1 fixed frequency wireless dual potentiostat system was used (Pinnacle Technology, Lawrence, KS, USA). The kit contained the Pinnacle 8151 wireless dual potentiostat, the voltage programmer, and a receiver base station (model 8106) with USB cables. Software for data acquisition (PAL) was also included in the kit. Biotransducers were interfaced with the 8151 wireless potentiostat via a custom connector. Two-electrode amperometric measurements of glucose or lactate was enabled, with the on-board working microelectrode array serving as the working electrode and the shorted on-board counter and reference electrodes serving as the counter electrode. A bias potential of 0.65 V was programmed into the 8151 and applied to the working electrode array of the MDEA 5037 with respect to the onboard counter electrode. To ensure functionality prior to implantation, *in vitro* calibration of MDEA 5037s was performed in PBS buffer at 37 ℃, within 8 h, prior to implantation. Steady state amperometric current produced was measured and the sensitivity of the device was determined from the slope of the calibration plot. *In vitro* calibrated sensitivity (S_o) was determined by the ratio of the resulting change in current density based on electrode geometric area to change in concentration of analyte in buffer in units of $\mu A \cdot cm^{-2} \cdot mM^{-1}$. Time dependent estimations of intramuscular glucose, $G_o(t)$ or lactate, $L_o(t)$ were made based on this reference sensitivity after implantation of the device. The kinetic parameters were determined using Lineweaver-Burk (LWB) analysis of biosensor amperometric dose response. The apparent Michaelis-Menten constant K_{Mapp} and the maximum current response, I_{max}, were calculated from the slope and the intercept of the Lineweaver-Burk plots [20,21]. Limits of detection were calculated by dividing 3*STDev (three times the standard deviation) of the steady-state, blank solution current response by the calculated sensitivity.

2.7. Implantation of Biotransducers into the Trapezius Muscles of Sprague-Dawley Rats

All animal studies were conducted under Clemson University IACUC Protocol # 2011-013, approved on 9 March, 2011, and valid through 8 March, 2014, under the supervision of Clemson University's

Institutional Animal Care and Use Committee (IACUC). Sprague-Dawley rats (250–450 g) were housed in plastic cages (1 rat/cage) at the Godley-Snell Research Center at Clemson University and kept on a 12 h light/dark cycle, with food and water provided *ad libitum*. Sprague-Dawley rats were shaved, sterilized, and placed under anesthesia on a warming pad. Throughout the biosensor implantation and evaluation experiments, the rats were maintained under anesthesia using 3% isoflurane flow. An incision was made above the trapezius muscle on the back to expose the fascia and muscle. Fascia was spread apart using blunt-tipped scissors to expose the muscle. A small pocket was formed by spreading the muscle tissue apart using microtweezers. The MDEA 5037 was carefully inserted into the pocket by hand. The muscle tissue was closed over the working region of the biotransducer and secured with a suture. Fascia was secured over the muscle tissue with a suture and the wound was closed with surgical staples. After implantation, the MDEA 5037 biotransducer was interfaced with the 8151 dual potentiostat and allowed to reach steady state for an hour. The rat was observed during this time to ensure stability.

2.8. In Vivo Biosensor Sensitivity and Response Time to Bolus Infusion of Analytes

After biosensor response reached a steady state baseline measurement of intramuscular analytes, measurements of blood analytes from the saphenous vein were made. Blood glucose was measured using a test-strip based Alpha TRAK glucose meter (Abbott Laboratories). A bolus of solution consisting of 3 M glucose and 0.4 M lactate prepared in 0.1 M PBS (pH = 7.4) was infused, up to 0.5 mL, through the tail vein. Procedures for measurement of interstitial analytes lasted for up to 3 h. One hour was used to allow the biosensors to reach a steady state. Blood analyte measurements and bolus infusions were made after reaching steady state and at 30 min intervals thereafter. Changes in amperometric response deviating from steady state were observed after the bolus injection of glucose and lactate into venous blood. Estimated interstitial analyte responses measured by biosensors calibrated *in vitro* were compared to analyte concentrations in the blood. Interstitial concentrations of glucose in non-diabetic rats have been shown to have a good 1:1 correlation to plasma glucose concentration at the basal state [43]. Sensitivity was determined based on *in vivo* responsiveness to exogenously changing levels of glucose and lactate. Rats were subsequently euthanized after procedures and the trapezius muscle surrounding the biotransducer was resected in order to safely recover biotransducers. Resected biotransducers were re-characterized *in vitro* to assess the functionality and lifetime of the device *in vivo*. Upon explantation the base current, sensitivity and response time of biosensors were once again evaluated in PBS at 37 ℃. Resected biotransducers were considered functional if sensitivity and maximum current were maintained, being not significantly different from freshly prepared sensors, can detect the physiologically relevant range of glucose or lactate, and have a response time of approximately 1 min.

3. Results and Discussion

3.1. Effects of a Polypyrrole Seeding Layer on Analytical Performance of Biotransducers

To create effective, stable and reproducible biotransducers, it is necessary to establish an intimate and stable interface between the biorecognition membrane layer and the underlying physicochemical

transducer, in this case, the metallic electrode. To achieve this, an approach has been developed that uses a nano-dimensioned seeding layer of electropolymerized, pristine, polypyrrole-polystyrene sulfonate. Electropolymerization serves as an additive fabrication process that places an organic electronic layer in intimate contact with an electrified metallic layer. No other surfaces of the device are affected. The effects of seeding transducers with PPy-PSSA prior to subsequent electropolymerization and entrapment of enzymes was explored. A low charge density of 10 mC/cm^2, corresponding to a film of 25 nm [28], was used as a seeding layer prior to applying 100 mC/cm^2 of PPy/GOx. Unseeded biotransducers, serving as a control, had a sensitivity of 0.77 (±0.35) μA·cm^{-2}·mM^{-1}, an I_{max} of 16.8 (±6.5) μA·cm^{-2}, a linear dynamic range maximum of 15.8 (±2.8) mM, a K_{Mapp} of 11.1 (±4.3) mM, and a limit of detection of 0.07 (±0.05) mM. Seeded biotransducers had a sensitivity of 1.44 (±0.78) μA·cm^{-2}·mM^{-1}, an I_{max} of 35.3 (±18.3) μA·cm^{-2}, a linear dynamic range maximum of 19.4 (±1.0) mM, a K_{Mapp} of 11.8 (±0.3) mM, and a limit of detection of 0.04 (±0.03) mM.

Figure 1 summarizes the effects of the PPy-PSSA seeding layer at 10 mC/cm^2 on the enzyme kinetic parameters of biotransducers fabricated at 100 mC/cm^2. Both the sensitivity and the apparent Michaelis-Menten enzyme kinetic parameters were statistically equivalent suggesting no deleterious influence of the adhesion promoting seeding layer on biotechnical performance. Both of the biotransducer types had much greater sensitivity to glucose in comparison to hydrogel coated biotransducers which have been reported to have a sensitivity of 0.045 μA·cm^{-2}·mM^{-1} [35]. Previous characterizations of unseeded immobilization of GOx with polypyrrole have yielded biotransducers with glucose sensitivity of approximately 0.6 μA·cm^{-2}·mM^{-1} which is similar to the results obtained in this body of work [38]. The linear range of an amperometric biosensor system is typically a function of analyte diffusivity through the bioactive membrane [44]. The linear dynamic range of seeded biotransducers was not significantly broader than that of unseeded biotrasducers. The nano-thin PPy-PSSA layer was not enough to serve as a barrier to diffusion of enzymatically generated hydrogen-peroxide in order to increase the linear range or adversely affect other enzyme kinetic parameters. The K_{Mapp} values determined show that no changes to enzyme affinity occurred as a result of the seeding layer. Seeded biotransducers showed less variability in K_{Mapp} indicating good reproducibility of enzyme affinity compared to unseeded transducers. For amperometric, enzyme-based biosensors, the maximum current is related to total enzyme activity [17]. The nearly 2-fold increase in maximum current was statistically significant (p = 0.045). These results are a good indication that the seeding layer serves to enhance loaded enzyme activity. It is likely that the seeding layer provides a surface that facilitates enzyme adsorption/entrapment without denaturation. Polypyrrole is known to have a stabilizing influence on enzymes [45]. Enzymes being immobilized onto an unseeded electrode will likely be entrapped within a mechanically disparate interface of Pt|PPy that may not preserve the structure of immobilized enzymes as effectively.

The principal role of the seeding layer was to significantly decrease the average biofabrication time from 68 (±22) min for the unseeded biotransducer to 35 (±6) min for the seeded biotransducer (p = 0.007); a reduction of 50%, and to improve reproducibility in biofabrication. Electropolymerization efficiency is an important biofabrication parameter. Enzymes require a hydrated, protective environment in order to function *in vivo*. Electropolymerization of pyrrole to entrap GOx within polypyrrole to yield a biosmart, pHEMA-based hydrogel has been used to fabricate *in vivo* biotransducers [46]. These hydrogels provided the necessary protective hosting of the immobilized biomolecules [47] and the

in vivo biocompatibility for the protection of the biotransducers [35]. However, hydrogel modified transducers require considerable overpotential for electropolymerization; as much as 1,000 mV *vs.* Ag/AgCl and the polymerization times are comparable to that of unmodified electrodes [35].

Figure 1. The effects of the PPy-PSSA seeding layer of 10 mC/cm^2 on the enzyme kinetic parameters of biotransducers fabricated using 100 mC/cm^2 (error bars show 95% confidence intervals, n ≥ 5). * = $p < 0.05$; ** = $p < 0.01$.

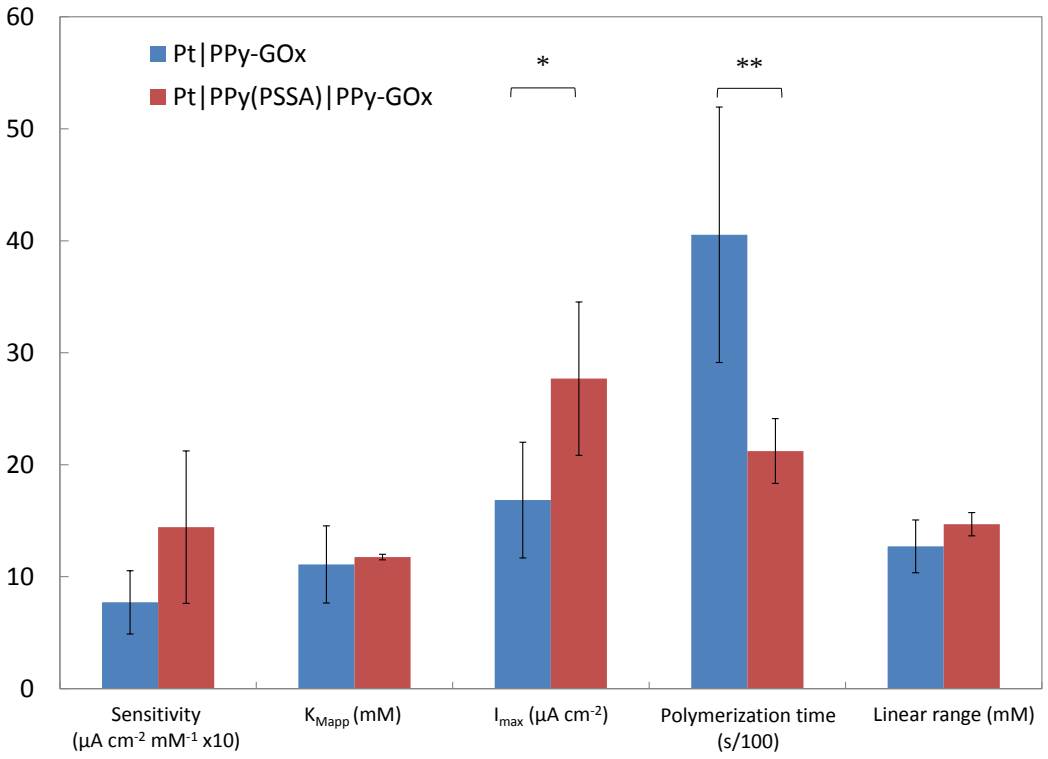

3.2. Enzyme Monomerization and Sulfonization

The monomerization of enzymes [48–51] and biomolecules [52,53] is a well-practiced art and the sulfonization of GOx using PEG spacer arms to a poly(2-acrylamido-2-methylpropane sulfonic acid) has likewise recently been described [54,55]. In this work, the amine groups of lysine residues of GOx were covalently coupled to either 4-(3-pyrrolyl)butyric acid or 4-sulfobenzoic acid using EDC-NHS coupling chemistry, Figure 2. The amperometric dose response of biotransducers to glucose was measured for (i) covalently conjugated systems: **PPy(SBA-*con*-GOx)**, **P(Py-*co*-PyBA-*con*-GOx)**, (ii) non-covalently conjugated systems: **PPy(SBA)-GOx**, **P(Py-*co*-PyBA)-GOx**, and (iii) control systems: **PPy-GOx**. The covalently conjugated systems with a 10:1 molecular ratio of PyBA:GOx or SBA:GOx are depicted in Figure 3.

The approach to covalent coupling considered in this work is intended to be a simple and effective means of enzyme conjugation that can be performed in a single solution and immediately used for electropolymerization without need for sophisticated separation steps. Moreover, these reactions are non-targeted, being potentially reactive with amine groups near the active site and with the potential for compromise of global enzyme structure and activity. It is noted that not all lysine groups will be available for conjugation and that the total number of lysine groups conjugated may likely be less than

that of the feed ratio. Monomerized enzymes were prepared with the intent of having them be directly incorporated into the backbone of the forming electropolymerized polypyrrole. Sulfonized enzymes were prepared in order to have them act as more effective dopants and so be more efficiently electrostatically entrapped within the growing layer of positively charged polypyrrole backbones.

Figure 2. Scheme of enzyme modification using EDC-NHS coupling chemistry to monomerize glucose oxidase with PyBA; Sulfonization of enzymes with SBA was performed in a similar fashion.

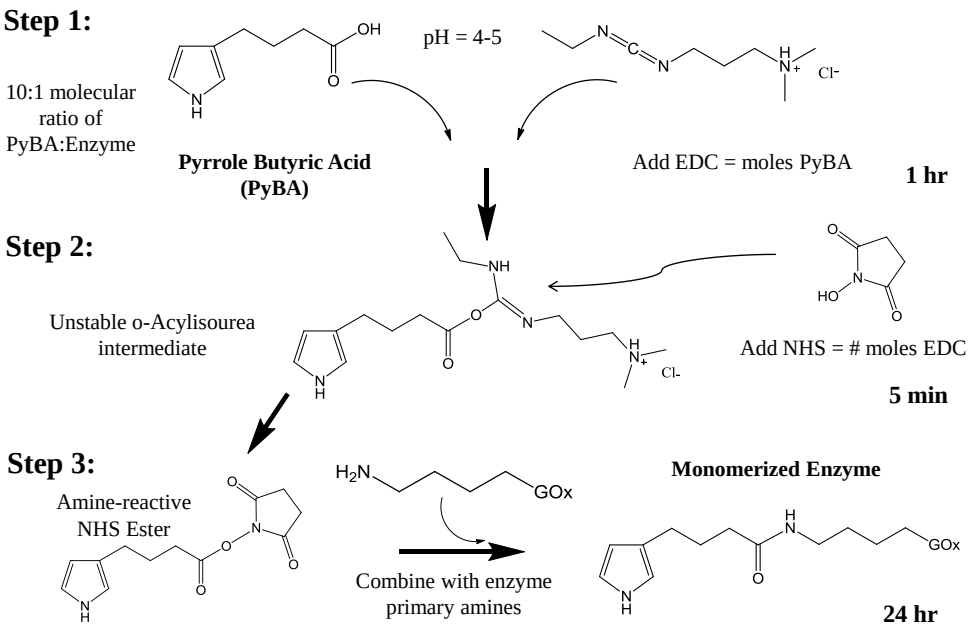

Figure 3. Subunit of glucose oxidase from *Aspergillus niger* with Lysine groups in red (**top**), monomerized enzymes used for preparing P(Py-*co*-PyBA-*con*-Gox) (**bottom left**) and sulfonated (**bottom right**) enzymes used for preparing PPy(SBA-*con*-GOx) with 10:1 ratio of PyBA or SBA conjugation to enzymes.

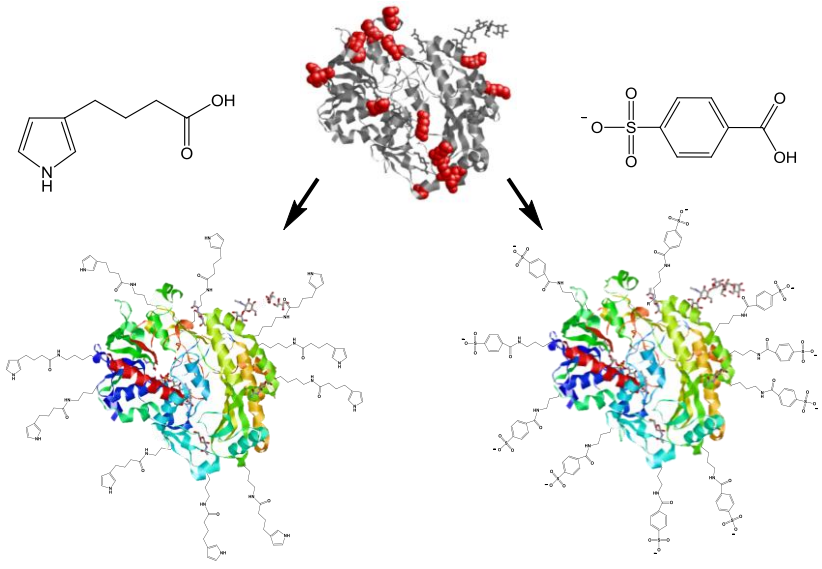

3.3. Electropolymerization Kinetics of Covalently Conjugated Systems

The kinetics of electropolymerization, defined as the time to reach 100 mC/cm^2 of charge, were compared for all systems studied. The control systems of PPy-GOx had an electropolymerization time of 68 ± 22 min. Enzyme systems containing PyBA, namely P(Py-*co*-PyBA)-GOx and P(Py-*co*-PyBA-*con*-GOx), both had significantly greater ($p < 0.03$) electropolymerization times compared to PPy-GOx. Enzyme systems PPy(SBA)-GOx, PPy(SBA-*con*-GOx) had significantly lower electropolymerization times compared to all other systems ($p < 0.02$). Sulfobenzoic acid is a highly mobile dopant capable of screening charge and making electropolymerization kinetics more facile for polypyrrole formation [56]. No significant difference in kinetics was noted between covalent and non-covalent conjugation for either PyBA or SBA systems. A decrease in variability in electropolymerization time was however observed for the covalently conjugated systems when compared to the non-covalently conjugated systems. There is likely some competition for doping sites within the formed polypyrrole between adsorbed glucose oxidase and PyBA/SBA in the non-covalent systems, whereas for covalently conjugated systems, the dopant becomes solely the adsorbed monomerized or sulfonated enzyme.

3.4. Characterization of Enzyme Conjugation using Ferrocene Monocarboxylic Acid

Cyclic voltammetry in the presence of a redox mediator, ferrocene monocarboxylic acid, was used to probe and confirm the extent of monomerization and sulfonization of enzymes by EDC-NHS coupling. A redox mediator, ferrocene monocarboxylic acid, was conjugated to glucose oxidase to a saturating extent using a 30:1 conjugation ratio of FcCOOH:GOx to confirm the effectiveness of covalent conjugation. In order to separate unreacted components of the solution after conjugation had taken place, samples were allowed to dialyze in a Slide-A-Lyzer dialysis cassette (Thermo Scientific Pierce, Rockford IL) in deionized water over night in a water bath, which was changed with fresh deionized water every 3 h. These samples are denoted as ‘Dialyzed’. After dialysis was complete the solutions were immediately characterized electrochemically. Cyclic voltammograms obtained at platinum microelectrodes in the presence of DI-water, unmodified GOx enzyme and covalently conjugated FcCONH-GOx enzyme is shown in Figure 4. The formal potential for ferrocene monocarboxylic acid is approximately 320 mV *vs*. Ag/AgCl [57]. Higher anodic and cathodic currents were observed for FcCOOH-GOx conjugates compared to just enzyme or DI-water. The oxidation and reduction peaks decreased for the conjugates after dialysis due to the removal of unreacted FcCOOH. Redox activity was still evident, however, indicating that covalent conjugation had occurred. Response from 1 mg/mL of GOx showed no changes and was identical to samples of GOx and FcCOOH mixed together without EDC/NHS and dialyzed (data not shown).

Figure 4. Cyclic voltammograms of GOx and FcCOOH-GOx covalent conjugates in DI-water at a scan rate of 50 mV/s.

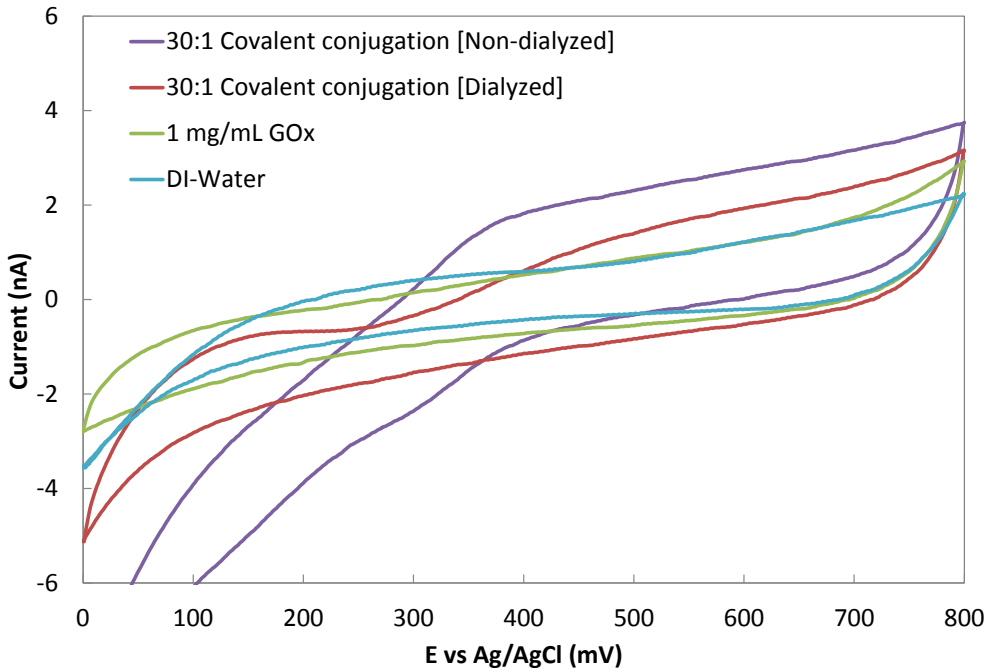

3.5. Bioanalytical Performance of Monomerized and Sulfonated Enzyme Biosensors

The dose response curves of biotransducers fabricated using monomerized GOx and sulfonated GOx are shown in Figure 5 and biosensor performance parameters for all systems are summarized in Table 1. The covalently sulfonated system, PPy(SBA-*con*-GOx), had a sensitivity of 1.92 ± 0.2 μA·cm^{-2}·mM^{-1}, a response time of 18 ± 5 s, a detection limit of 2.2 × 10^{-3} ± 1.8 × 10^{-3} mM, a K_{Mapp} of 11.1 ± 5.6 mM, a maximum current of 39.2 ± 11.7 μA·cm^{-2} and a linear dynamic range of 10.2 ± 3.2 mM. The PPy(SBA-*con*-GOx) system was significantly more sensitive ($p < 0.0002$) than the PPy-GOx system. The PPy(SBA-*con*-GOx) system was shown to have the best limits of detection with significantly better ($p = 0.002$) resolution compared to P(Py-*co*-PyBA-*con*-GOx). Response times were equivalent among all systems. The non-covalently coupled SBA system, PPy(SBA)-GOx, had a sensitivity of 1.8 ± 1.2 μA·cm^{-2}·mM^{-1} which was found to be the same as PPy-GOx controls. Electropolymerized polypyrrole glucose biotransducers fabricated with GOx conjugated to poly(2-acrylamido-2-methylpropane sulfonic acid) polyanion dopants have been shown to have sensitivity ranging from 180–270 nA/mM/cm^2 with a linear range of 20–26 mM and a Michaelis-Menten constant of 46.7 mM [55,58]. Overall the covalent sulfonization process successfully yielded biotransducers with higher sensitivity but at the cost of decreased linear dynamic range when compared to the GOx-polyanion system found in the literature. Biotransducers were able to maintain unchanged functionality for up to 8 days with storage in PBS at 4 ℃. After the 8-day period background current increased and sensitivity decreased during characterization in PBS (data not shown).

Table 1. Dose response (PBS, pH = 7.2, 25 ℃) performance parameters for biotransducers fabricated with (10:1 ratio PyBA/SBA:GOx) covalently modified enzymes, non-covalently modified enzymes and control systems having no modification (±standard deviation is shown).

[E] = 1.0 mg/mL	PPy-GOx (n = 4)	PPy(SBA)-GOx (n = 4)	PPy(SBA-*con*-GOx) (n = 2)	P(Py-*co*-PyBA)-GOx (n = 2)	P(Py-*co*-PyBA-*con*-Gox) (n = 2)
Polymerizaton time (R.L. 100 mC/cm^2) (min)	68 ± 22	23 ± 19	15 ± 5	204 ± 37	230 ± 132
Sensitivity (μA·cm^{-2}·mM^{-1})	0.87 ± 0.04	1.8 ± 1.2	1.9 ± 0.2	4.8 ± 0.9	0.99 ± 0.28
Response time (s)	41 ± 21	17 ± 9	18 ± 5	17 ± 5	14 ± 5
Detection limit (mM)	0.5 ± 0.3	0.01 ± 0.01	2.2 × 10^{-3} ± 1.8 × 10^{-3}	0.05 ± 0.03	0.02 ± 0.01
K_{Mapp} (mM)	14.1 ± 3.1	8.2 ± 2.6	11.1 ± 5.6	7.2 ± 2.6	19.7 ± 3.9
I_{max} (μA·cm^{-2})	23.3 ± 3.1	30.6 ± 18.8	39.2 ± 11.7	77 ± 25	28.9 ± 4.0
Linear range (mM)	17.4 ± 7.0	9.4 ± 2.6	10.2 ± 3.2	9.5 ± 2.8	25.6 ± 5.6

Figure 5. Dose response curves of (**left**) monomerized and (**right**) sulfonated enzyme biotransducers prepared on Pt|PPy-PSSA seeding layers of 10 mC/cm^2 at ϕ = 100 μ·Pt·μE.

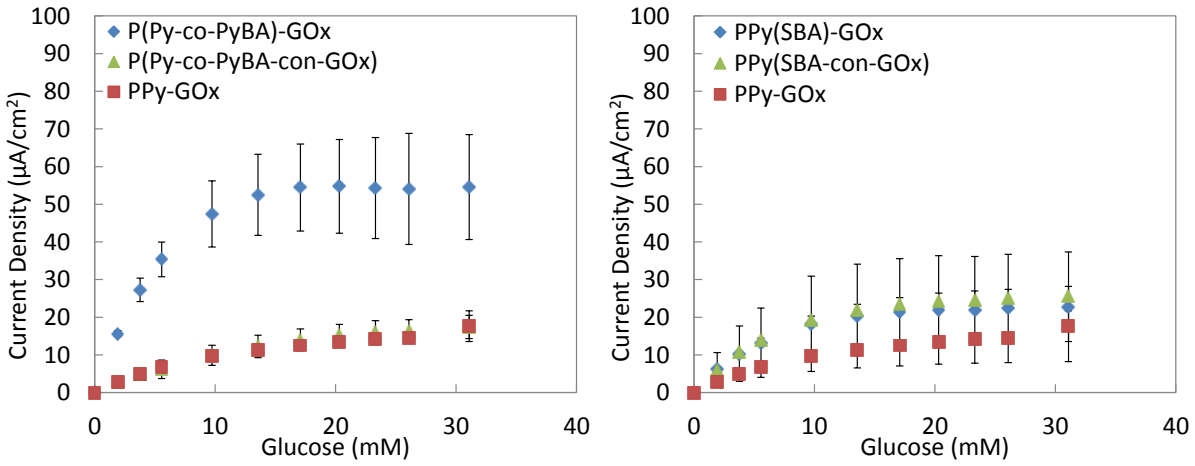

The non-covalently conjugated system, P(Py-*co*-PyBA)-GOx, had a sensitivity of 4.8 ± 0.9 μA·cm^{-2}·mM^{-1}, a response time of 17 ± 5 s, a detection limit of 0.05 ± 0.03 mM, a K_{Mapp} of 7.2 ± 2.6, a maximum current of 77 ± 25 μA·cm^{-2} and a linear range of 9.5 ± 2.8 mM. Its sensitivity was significantly greater than every other biotransducer (p < 0.045) except the sulfonated system, PPy(SBA-*con*-GOx). P(Py-*co*-PyBA)-GOx had the highest maximum current of all systems studied and was significantly greater (p < 0.01) than the PPy-GOx system. Covalently monomerized GOx did not perform statistically different from PPy-GOx. Glucose oxidase that is lysyl modified with an N-substituted 1H-Pyrrole-1-propionic acid has been shown to have higher electrode activity compared to native GOx in polypyrrole membranes [59]. Chemical modification of GOx lysine groups with 3-carboxymethyl pyrrole has also been shown to exhibit higher enzyme activity and storage stability than systems using N-substituted pyrrole [60]. Our results show that incorporation of PyBA without covalent coupling is sufficient for increasing biosensor performance with respect to higher sensitivity and overall enzyme activity without the need to modify electrode geometry or properties. Enhancing

surface area of the electrode through use of nanofeatures can improve sensitivity by an order of magnitude, 10 $\mu A \cdot cm^{-2} \cdot mM^{-1}$ [61]. This improvement, however, may not carry over to the final *in vivo* biosensor system which will be coated with bioactive hydrogels that is expected to limit diffusion [35,62].

The MDEA 5037 system was equal in performance with respect to response time and improved in performance with respect to sensitivity when compared to wire-type epoxy-polyurethane implantable systems which have been shown to have response times ranging from 20–200 s with sensitivity ranging from 1–6 nA/mM [63]. Rapid response is necessary for these implantable systems in order to most accurately report physiological conditions *in vivo*. For enzyme-based amperometric biosensors, the response time will generally be limited by the diffusion of glucose and hydrogen peroxide through the bioactive polymer membrane. Spin casting hydrogels to control thickness of bioactive membranes can be used to ensure that effective response times (<60 s) are maintained. Linearity of response for these enzyme-modified systems was generally similar to that of biosensors fabricated with GOx entrapped by composites of nanoparticles and polypyrrole with limits between 4 and 13 mM [64–66]. Linear range limits of 20 mM have been achieved using PPy coated gold nanoparticles, an increase which comes with decreased sensitivity by a factor of 6 and increased K_{Mapp} [67]. Similar types of observations were made for the covalently monomerized biotransducer system, wherein sensitivity decreased by an order of about 4–5 while increases in K_{Mapp} and linear range occurred. A high linear range is valuable for accurate measurement of high concentrations of glucose without the need for estimation from curve fits. Carbon nanotube doped polypyrrole, when used to entrap GOx onto a glassy carbon electrode, can reach a linear range of up to 50 mM but with compromised sensitivity of 2.3 nA/mM [68].

3.6. Effect of Extent of Monomerizaton or Sulfonation

The extent of monomerization and sulfonation and its impact on biosensor sensitivity was examined by varying the ratio of PyBA and SBA conjugated to glucose oxidase, Figure 6. A ratio of 2:1 was compared to 10:1. Sensitivity decreased as conjugation increased for monomerized enzymes and increased for sulfonated enzymes. A significant decrease in sensitivity from 4.8 ± 0.9 $\mu A \cdot cm^{-2} \cdot mM^{-1}$ at 0:1 conjugation to 0.1 ± 0.01 $\mu A \cdot cm^{-2} \cdot mM^{-1}$ at 2:1 conjugation ($p = 0.02$) and 1.0 ± 0.3 $\mu A \cdot cm^{-2} \cdot mM^{-1}$ at 10:1 conjugation ($p = 0.03$) was noted for the monomerized systems. For sulfonated systems sensitivity significantly increased from 1.0 ± 0.03 $\mu A \cdot cm^{-2} \cdot mM^{-1}$ at 0:1 conjugation to 1.7 ± 0.5 $\mu A \cdot cm^{-2} \cdot mM^{-1}$ at 2:1 conjugation ($p = 0.03$) and 1.9 ± 0.2 $\mu A \cdot cm^{-2} \cdot mM^{-1}$ at 10:1 conjugation ($p < 0.0002$). Monomerized GOx systems had sluggish electropolymerization kinetics with long times required to reach 100 mC/cm^2 of charge density. This would allow a greater number of enzymes to adsorb onto the forming polypyrrole during the polymerization process resulting in a higher sensitivity for the system.

The conjugation to PyBA is likely affecting the active sites of the enzymes leading to the overall decreased sensitivity. The sensitivity increased after increasing the conjugation from 2:1 to 10:1, which may be due to more enzymes being directly incorporated into the polypyrrole network through the enzyme conjugation process. Sulfonated enzymes had the most rapid electropolymerization kinetics, the result of the SO_3^- highly effective dopant. The monotonically increasing sensitivity for sulfonated enzymes suggests that electrostatic interactions are likely playing a key role in enzyme immobilization via electropolymerization. The contents of the enzyme-monomer solution used for electropolymerization

will largely dictate the polymer structure, morphology, thickness, conductance, and biosensor performance parameters [69,70]. The non-covalent and covalent conjugated enzymes in this work were designed with the intent to maximize biotransducer enzyme content by having the enzymes dope the forming polypyrrole. This was shown to have a significant influence on the kinetics of polymerization and improvements in sensitivity, maximum current, and linear range. However, these improvements were achieved with limited reproducibility. The same charge density was maintained throughout PPy film production but was likely limited and affected by the low current densities observed during fabrication, which would have caused differences in film thickness and morphology. Optimization of the electrolyte or dopant composition of the electropolymerization solution will be necessary in the future to improve the quality of the polypyrrole films produced and thereby improve the bioanalytical reproducibility among biotransducers. For the preliminary characterization of intramuscularly implanted biosensor systems each biotransducer was characterized and calibrated individually prior to use.

Figure 6. Effects of the extent of monomerization and sulfonization via increasing molecular ratio of PyBA or SBA to GOx on biosensor sensitivity.

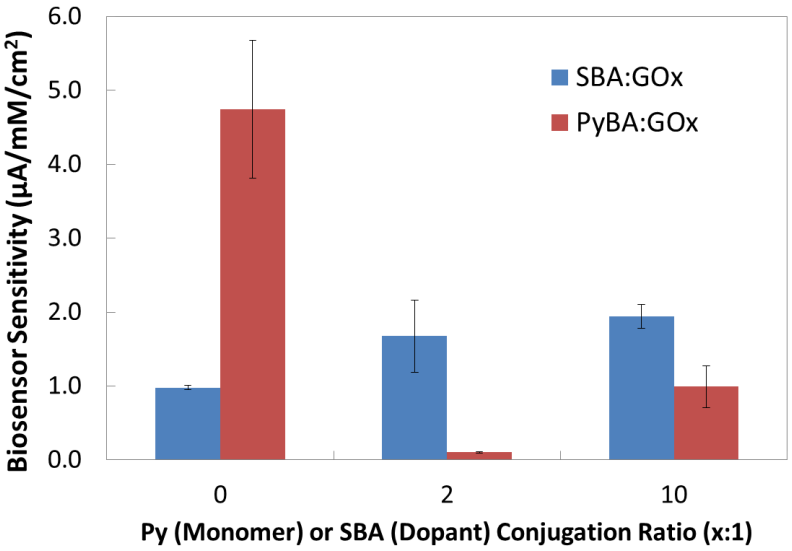

3.7. Performance of Freshly Prepared and Resected Biotransducers

Biotransducers fabricated using the MDEA 5037-Pt platform were characterized immediately after their fabrication and again immediately following resection from the trapezius muscle of Sprague-Dawley rats. Figure 7 shows the dose–response curves and performance parameters of glucose biosensors fabricated using glucose oxidase, an FAD-based enzyme, before and after resection. The biosensors varied in terms of their performance and, thus, were calibrated independently prior to use *in vivo*. Table 2 summarizes the key bioanalytical performance characteristics of the biotransducers before and after resection. The MDEA 5037 biotransducers were implanted in muscle tissue for up to 3 h. The overall performance of resected biotransducers was diminished compared to when they were freshly prepared which was expected.

Figure 7. (**A**) Dose response of MDEA 5037-Pt biotransducers to glucose with enzyme concentration used for fabrication shown in parentheses, and (**B**) Bioanalytical performance of glucose biosensors after being freshly fabricated and following resection from rat trapezius muscle (650 mV bias, PBS buffer, pH = 7.2, 25 ℃, ±standard deviation is shown).

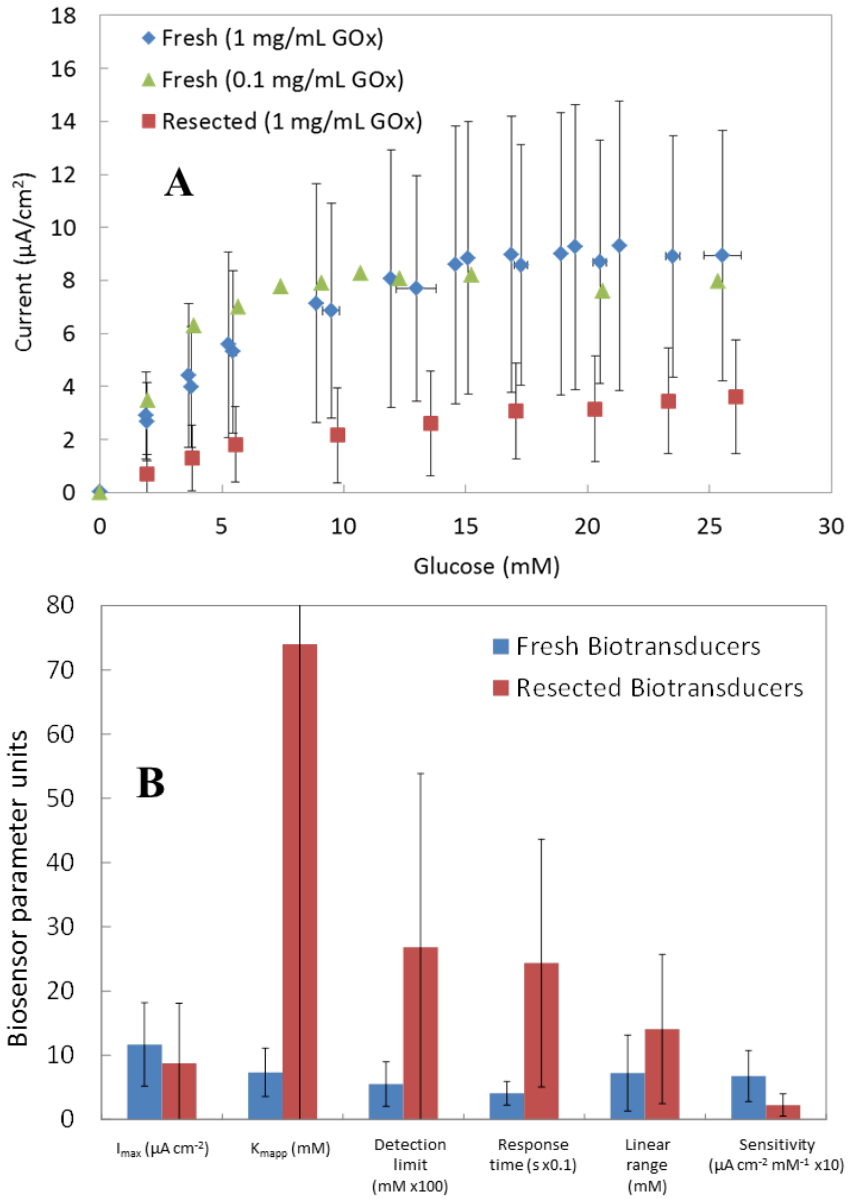

Lactate biotransducers did not produce adequate current densities in response to *in vitro* lactate challenge to be considered for *in vivo* analysis when paired with the Pinnacle 8151 wireless dual-potentiostat. The lactate sensors had a good sensitivity of 0.36 ± 0.15 $\mu A \cdot cm^{-2} \cdot mM^{-1}$ and a linear dynamic range of 6.6 ± 0.9 mM. Based on the observed I_{max} and K_{Mapp} the lactate biosensors did not adhere well to L-B analysis. Given the detection limits of 7.9 ± 5.6 mM, currently fabricated lactate biotransducers could only accurately discern changes in interstitial lactate corresponding to extremes of hyperlactatemia (Δ[lactate] > 4 mM) [71,72]. Glucose biotransducers showed diminished sensitivity after use *in vivo*, a decrease from 0.68 ± 0.40 to 0.22 ± 0.17 $\mu A \cdot cm^{-2} \cdot mM^{-1}$ (p = 0.08), and an increase in response time, which increased from 41 ± 18 to 244 ± 193 s (p = 0.08). The detection limit increased from 0.05 ± 0.03 to 0.27 ± 0.27 mM (p = 0.17), K_{Mapp} increased from 7.3 ± 3.4 to 74 ± 130 mM

(p = 0.35), I_{max} decreased from 11.7 ± 6.5 to 8.8 ± 9.3 (p = 0.30), and the linear range increased from 7.2 ± 5.9 to 14.1 ± 11.6 (p = 0.34).

Table 2. Bioanalytical performance parameters for lactate and glucose responsive biotransducers, freshly fabricated and following resection after 3 h of implantation in the trapezius muscle of Sprague-Dawley rats (650 mV bias, PBS, pH = 7.2, 25 ℃, ±standard deviation is shown).

	MDEA 5037-Pt|PPy(PSSA)|p(Py-*co*-PyBA)-LOx [E] = 1.0 mg/mL		**MDEA 5037-Pt|PPy(PSSA)|p(Py-*co*-PyBA)-GOx [E] = 1.0 mg/mL**	
	Freshly prepared biotransducers (n = 3)	**Resected biotransducers (n = 3)**	**Freshly prepared biotransducers (n = 4)**	**Resected biotransducers (n = 4)**
Sensitivity ($\mu A \cdot cm^{-2} \cdot mM^{-1}$)	0.36 ± 0.15	-	0.68 ± 0.40	0.22 ± 0.17
Response time (s)	86 ± 26	-	41 ± 18	244 ± 193
Detection limit (mM)	7.9 ± 5.6	-	0.05 ± 0.03	0.27 ± 0.27
K_{Mapp} (mM)	−9.1 ± 15.8	-	7.3 ± 3.4	74 ± 130
I_{max} ($\mu A\ cm^{-2}$)	−1.9 ± 5.8	-	11.7 ± 6.5	8.8 ± 9.3
Linear range (mM)	6.6 ± 0.9	-	7.2 ± 5.9	14.1 ± 11.6

Implanted biotransducers may demonstrate compromised performance due to component-based and biocompatibility-based failures [73]. The following mechanisms of failure for the explanted biosensors were analyzed: lead detachments, electrical shorts, component delamination and degradation, biofouling, electrode passivation, and fibrous encapsulation. Biotransducers were exposed to whole blood and the possibility of protein adsorption, as well as the reactive oxygen species of the acute inflammatory response during their period of implantation. The dramatic increase in response time and K_{Mapp} is likely due to the effect of proteins being adsorbed from surrounding tissue, plasma, and interstitial fluid to the biotransducer surface. Protein adsorption has been shown to have a negative influence on glucose diffusion for implantable and continuous biosensor systems [74,75]. However, no physical deterioration of the MDEA 5037 transducer was observed and none of the resected biotransducers had spurious responses indicating that neither instrumentation problems nor transducer compromises were causing the changes in performance. Limits of detection were maintained at adequate levels to discern changes in glucose using the biosensor system. Production of hydrogen peroxide has been identified as the main agent for short-term enzyme degradation *in vivo* [76]. The lack of significant change in maximum current shows that the original enzyme activity was still present in the system after short-term use *in vivo*, supporting these previous findings. Overall, the MDEA 5037 biotransducers maintained their activity after short-term implantation with respect to sensitivity, maximum current, range of response, and response time.

3.8. In Vivo Response of MDEA 5037 Biotransducers to Exogenously Changing Analytes

Three dual responsive MDEA 5037-Pt|PPy(PSSA)|p(Py-*co*-PyBA)-GOx(Ch1)-Pt|PPy(PSSA)|p(Py-*co*-PyBA)-LOx(Ch2) biotransducers were tested *in vivo* (MDEA-1, MDEA-2 and MDEA-3). Figure 8 shows the implanted biotransducer within the trapezius muscle of Sprague-Dawley rats under anesthesia.

Figure 8. Sprague-Dawley rat under anaesthesia with, (**A**) the MDEA 5037 biotransducer implanted into trapezius muscle and secured into place with a suture, and (**B**) the incision closed and secured around the MDEA 5037 with surgical staples.

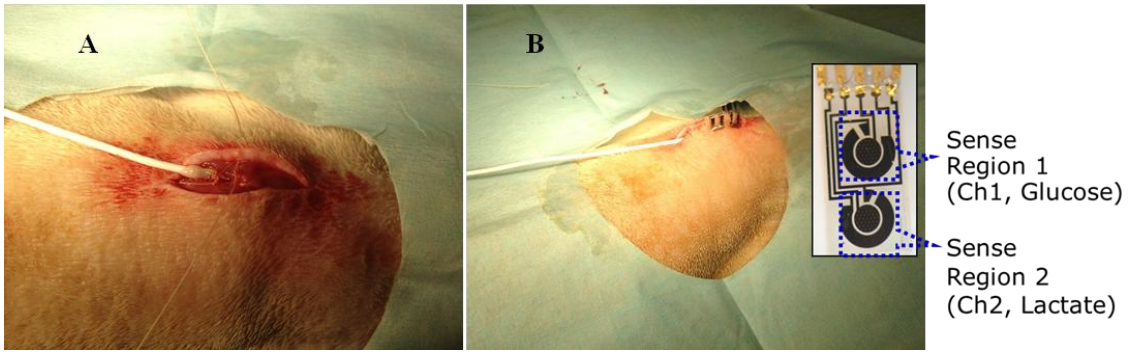

Following implantation, devices were allowed to stabilize and steady state currents were established and sustained for approximately 1 h. The average blood glucose and amperometric *in vivo* responses of the glucose sensitive channels are shown in Figure 9. MDEA-1 and MDEA-3 were prepared having a glucose sensitive cell (Channel 1) and a lactate sensitive cell (Channel 2). Response of Channel 2 for these biotransducers was omitted for clarity. MDEA-2 utilized two glucose sensitive cells (Channels 1 and 2) to compare differences in response to glucose on the same biotransducer. Intramuscular glucose via the biosensor was compared to venous blood glucose collected from the saphenous vein and measured with the Alpha TRAK. The first sensor, MDEA-1, came to a stable base-line current, and interstitial glucose concentrations did not vary much between 1.91–2.23 mM. This seemed reasonable as blood glucose did not vary, remaining between 5.49–5.88 mM. One of the sensors (MDEA-2, Channel 2) showed a sustained increase in interstitial glucose after tail vein infusions of glucose. For the case of MDEA-2, both channels were sensitive to glucose. However, only one of the channels (Channel 2) showed a change in interstitial glucose while the other (Channel 1) did not. MDEA-3 showed a decreasing trend of interstitial glucose concentration with a rapid increase and subsequent fall within minutes after a tail vein infusion.

Glucose measurements made using the intramuscularly implanted MDEA 5037 biosensors and the whole blood Alpha TRAK handheld were compared, Figure 10. Intramuscular glucose measurements were consistently lower than blood glucose measurements. Previous comparisons of blood *versus* interstitial glucose concentrations in humans have indicated that as blood glucose increases interstitial values will increase at a slower rate with a total lag of 17.2 ± 7.2 min [77]. Glucose concentrations have been shown to change significantly faster in the blood of anesthetized rats with a rate of 6.8 ± 2.0 mg/dL/min compared to subcutaneous fluid having a rate of 3.9 ± 1.3 mg/dL/min [78]. For rats given an infusion of insulin the difference between subcutaneous glucose and blood glucose has been shown to vary from 30% to 120% within the first 30 min [78]. Thus, we can expect to see major differences between compartments in the anesthetized rats receiving large boluses of glucose and lactate. We should expect to see some similarities between blood and interstitial glucose concentrations at the basal level. Tissue contact after implantation likely played a role in response after implantation. Short-duration implantations, such as these, do not provide sufficient time for tissue remodelling to allow sustained intimate contact between the host tissues and the biotransducer surface [79,80]. Longer implantation times will be incorporated in the future. In addition to this, a more

gradual ramp administration of glucose will be used. This technique has been shown to yield more rapid and accurate sensor response and a more physiologically relevant response in animals [80,81]. Another drawback of this preliminary study is that the diet, size, and gender of the rats were not controlled.

Figure 9. Average whole blood and intramuscular (biosensor, 650 mV) glucose response at 30 min intervals after reaching steady state in the trapezius muscle of MDEA-1 in a male Sprague-Dawley rat of 412 g, MDEA-2 in a male Sprague-Dawley rat of 408 g and MDEA-3 in a female Sprague-Dawley rat of 265 g (infusions were of 3 M glucose in PBS, error bars show standard deviation of $n \geq 2$).

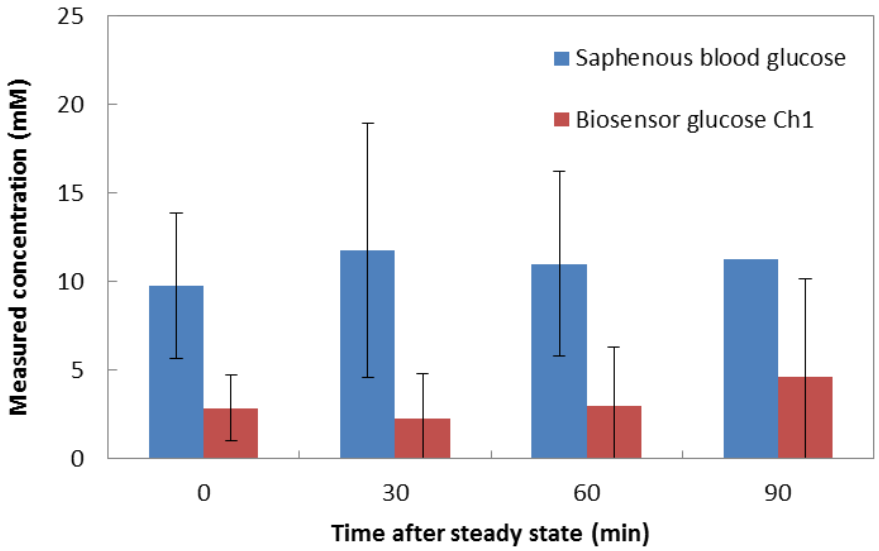

Figure 10. Response comparison of the implanted MDEA 5037 glucose biotransducers with respect to hand-held Alpha TRAK measurement of venous blood glucose as a reference.

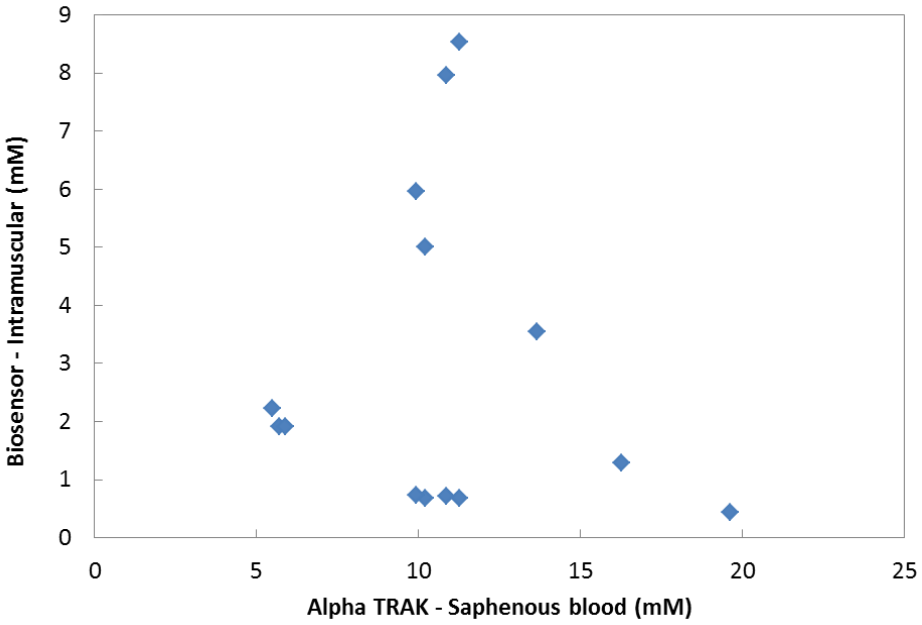

Background current could not be fully accounted for with these biotransducers as both electrochemical channels were used for simultaneous dual analyte detection. Accuracy in continuous monitoring can be improved by ratiometrically correcting for background current [82]. Background current stability of biosensors is known to display drift *in vivo* [83]. Future studies will need to take into consideration background current immediately prior to implantation. Electroconductive hydrogel modified biotransducers will also be used in future studies, which will likely have better stability *in vivo* compared to just polypyrrole modified biotransducers. The biosmart hydrogels have been shown to mitigate protein adsorption [62] which may lead to better short-term performance *in vivo*. The inclusion of hydrogels will be necessary for the protection of enzymes and mitigation of fibrous encapsulation for long-term implantation of biosensors.

4. Conclusions

Platinum microelectrodes seeded with a PPy-PSSA layer prior to additive electropolymerization of a PPy-enzyme layer had no significant effect on biotransducer sensitivity, linear dynamic range, limits of detection and response time but served to increase maximum current and reduce biofabrication time. These results indicate that entrapping enzymes onto polypyrrole seeded electrodes better maintains activity compared to entrapment directly onto the electrodes. Seeded transducers also had significantly more facile polypyrrole electropolymerization kinetics. The seeding layer may be a good option for making the polymerization kinetics more facile; with a smaller overpotential in these hydrogel systems when highly mobile dopants (Cl^-, HPO_4^{2-}) are not available. Sulfonization of enzymes was shown to be a fast and an effective means of improving biotransducer performance. Sulfonization using sulfobenzoic acid at a 10:1 SBA:GOx ratio was shown to be useful in making electropolymerization kinetics more facile and doubling biotransducer sensitivity compared to native enzyme systems. Monomerization of enzymes using pyrrole butyric acid at a 10:1 PyBA:GOx ratio did not significantly influence biotransducer performance, however, non-covalently incorporated pyrrole butyric acid dramatically increased biotransducer sensitivity and decreased linear dynamic range. This increase may be due to an increased number of adsorbed enzymes during electropolymerization.

The MDEA 5037 biotransducers and Pinnacle 8151 wireless dual potentiostat biosensor system was successfully prepared and characterized *in vivo*. Both, glucose and lactate biosensors were prepared and characterized *in vitro* prior to implantation. Lactate biosensor performance was insufficient for characterization *in vivo* as the limit of detection was not low enough. Glucose biosensors performed as expected based on previous characterization *in vitro*. MDEA 5037 biotransducers maintained full functionality after 3 h of implantation in the trapezius muscle of Sprague-Dawley rats. No significant decreases in sensitivity and maximum current were observed after biotransducers were resected. Protein adsorption onto the MDEA 5037 biotransducer surface after short-term use *in vivo* is likely the cause for dramatically increased response time and increased K_{Mapp}. To improve both short-term and long-term performance *in vivo*, the biotransducers will need to be coated with a biocompatible hydrogel layer that can mitigate protein adsorption. Likewise, background current will also need to be reduced.

Acknowledgments

This work was supported by the US Department of Defense (DoDPRMRP) grant PR023081/ DAMD17-03-1-0172, by the Consortium of the Clemson University Center for Bioelectronics, Biosensors and Biochips (C3B) and by ABTECH Scientific, Inc.

Author Contributions

C.N.K. performed most experiments and contributed writing, O.K. performed some experiments, and A.G-E. designed experiments, supervised the work, and contributed to writing.

Conflicts of Interest

The authors declare no conflict of interest.

References

1. Park, J.; Kim, C.S.; Choi, M. Oxidase-coupled amperometric glucose and lactate sensors with integrated electrochemical actuation system. *IEEE Trans. Instrum. Meas.* **2006**, *55*, 1348–1355.
2. Kotanen, C.; Guiseppi-Elie, A. Characterization of a wireless potentiostat for integration with a novel implantable biotransducer. *IEEE Sens. J.* **2013**, *14*, 768–776.
3. Zimmermann, S.; Fienbork, D.; Flounders, A.W.; Liepmann, D. In-device enzyme immobilization: Wafer-level fabrication of an integrated glucose sensor. *Sens. Actuator B Chem.* **2004**, *99*, 163–173.
4. Endo, H.; Yonemori, Y.; Hibi, K.; Ren, H.; Hayashi, T.; Tsugawa, W.; Sode, K. Wireless enzyme sensor system for real-time monitoring of blood glucose levels in fish. *Biosens. Bioelectron.* **2009**, *24*, 1417–1423.
5. Uyehara, C.F.T.; Sarkar, J. Role of vasopressin in maintenance of potassium homeostasis in severe hemorrhage. *Am. J. Physiol. Regul. Integr. Comp. Physiol.* **2013**, *305*, R101–R103.
6. Bartlett, P.N.; Whitaker, R.G. Electrochemical immobilisation of enzymes: Part I. Theory. *J. Electroanal. Chem. Interfacial Electrochem.* **1987**, *224*, 27–35.
7. Bartlett, P.N.; Whitaker, R.G. Electrochemical immobilisation of enzymes: Part II. Glucose oxidase immobilised in poly-*N*-methylpyrrole. *J. Electroanal. Chem. Interfacial Electrochem.* **1987**, *224*, 37–48.
8. Sadki, S.; Schottland, P.; Brodie, N.; Sabouraud, G. The mechanisms of pyrrole electropolymerization. *Chem. Soc. Rev.* **2000**, *29*, 283–293.
9. Yehezkeli, O.; Yan, Y.-M.; Baravik, I.; Tel-Vered, R.; Willner, I. Integrated oligoaniline-cross-linked composites of Au nanoparticles/glucose oxidase electrodes: A generic paradigm for electrically contacted enzyme systems. *Chem. Eur. J.* **2009**, *15*, 2674–2679.
10. Bai, J.; Beyer, S.; Trau, D. 3.331. Conjugated polymers for biosensor devices. In *Comprehensive Biomaterials*; Ducheyne, P., Ed.; Elsevier: Oxford, UK, 2011; pp. 529–556.
11. Palmisano, F.; Centonze, D.; Zambonin, P.G. An *in situ* electrosynthesized amperometric biosensor based on lactate oxidase immobilized in a poly-o-phenylenediamine film: Determination of lactate in serum by flow injection analysis. *Biosens. Bioelectron.* **1994**, *9*, 471–479.

12. Zhou, H.; Chen, H.; Luo, S.; Chen, J.; Wei, W.; Kuang, Y. Preparation and bioelectrochemical responses of the poly(m-phenylenediamine) glucose oxidase electrode. *Sens. Actuator B Chem.* **2004**, *101*, 224–230.
13. Badea, M.; Curulli, A.; Palleschi, G. Oxidase enzyme immobilisation through electropolymerised films to assemble biosensors for batch and flow injection analysis. *Biosens. Bioelectron.* **2003**, *18*, 689–698.
14. Bartlett, P.N.; Caruana, D.J. Electrochemical immobilization of enzymes. Part V. Microelectrodes for the detection of glucose based on glucose oxidase immobilized in a poly(phenol) film. *Analyst* **1992**, *117*, 1287–1292.
15. Bartlett, P.N.; Caruana, D.J. Electrochemical immobilization of enzymes. Part VI. Microelectrodes for the detection of L-lactate based on flavocytochrome b2 immobilized in a poly(phenol) film. *Analyst* **1994**, *119*, 175–180.
16. Tseng, T.T.-C.; Yao, J.; Chan, W.-C. Selective enzyme immobilization on arrayed microelectrodes for the application of sensing neurotransmitters. *Biochem. Eng. J.* **2013**, *78*, 146–153.
17. Karunwi, O.; Wilson, A.N.; Kotanen, C.N.; Guiseppi-Elie, A. Engineering the abio-bio interface to enable more than moore in functional bioelectronics. *J. Electrochem. Soc.* **2013**, *160*, B60–B65.
18. Apetrei, C.; Rodríguez-Méndez, M.L.; De Saja, J.A. Amperometric tyrosinase based biosensor using an electropolymerized phosphate-doped polypyrrole film as an immobilization support. Application for detection of phenolic compounds. *Electrochimica Acta* **2011**, *56*, 8919–8925.
19. Palmisano, F.; Zambonin, P.G.; Centonze, D. Amperometric biosensors based on electrosynthesised polymeric films. *Fresenius J. Anal. Chem.* **2000**, *366*, 586–601.
20. Guiseppi-Elie, A. Chemical and Biological Sensor Devices Having Electroactive Polymer Thin Films Attached to Mirofabricated Devices and Possessing Immobilized Indicator Moieties. U.S. Patent No. 5,766,934, 1998.
21. Guiseppi-Elie, A.; Brahim, S.; Wilson, A.M. Biosensors based on electrically conducting polymers. In *Handbook of Conducting Polymers: Conjugated Polymer Processing and Applications*, 3rd ed; Skotheim, T., Reynolds, J.R., Eds.; Taylor and Francis: New York, NY, USA, 2007; Volume 2, pp. 12:11–12:45.
22. Cosnier, S. Biomolecule immobilization on electrode surfaces by entrapment or attachment to electrochemically polymerized films. A review. *Biosens. Bioelectron.* **1999**, *14*, 443–456.
23. Valaski, R.; Ayoub, S.; Micaroni, L.; Hümmelgen, I. Influence of film thickness on charge transport of electrodeposited polypyrrole thin films. *Thin Solid Films* **2002**, *415*, 206–210.
24. Lee, H.; Yang, H.; Kwak, J. Dependence of the electrochemical behavior of poly(N-phenylpyrrole) films on the type of anion and solvent used in the electropolymerization. *J. Phys. Chem. B* **1999**, *103*, 6030–6035.
25. Lee, H.; Yang, H.; Kwak, J. Effects of dopant anions and *N*-substituents on the electrochemical behavior of polypyrrole films in propylene carbonate solution. *Electrochem. Comm.* **2002**, *4*, 128–133.
26. Tseng, T.T.-C.; Monbouquette, H.G. Implantable microprobe with arrayed microsensors for combined amperometric monitoring of the neurotransmitters, glutamate and dopamine. *J. Electroanal. Chem.* **2012**, *682*, 141–146.

27. Kotanen, C.; Guiseppi-Elie, A. Development of an implantable biosensor system of physiological status monitoring during long duration space exploration. *Gravit. Space Biol.* **2011**, *23*, 55–64.
28. Holdcroft, S.; Funt, B.L. Preparation and electrocatalytic properties of conducting films of polypyrrole containing platinum microparticulates. *J. Electroanal. Chem. Interfacial Electrochem.* **1988**, *240*, 89–103.
29. George, P.M.; Lyckman, A.W.; LaVan, D.A.; Hegde, A.; Leung, Y.; Avasare, R.; Testa, C.; Alexander, P.M.; Langer, R.; Sur, M. Fabrication and biocompatibility of polypyrrole implants suitable for neural prosthetics. *Biomaterials* **2005**, *26*, 3511–3519.
30. Wang, X.; Gu, X.; Yuan, C.; Chen, S.; Zhang, P.; Zhang, T.; Yao, J.; Chen, F.; Chen, G. Evaluation of biocompatibility of polypyrrole *in vitro* and *in vivo*. *J. Biomed. Mater. Res. A* **2004**, *68A*, 411–422.
31. Ramanaviciene, A.; Kausaite, A.; Tautkus, S.; Ramanavicius, A. Biocompatibility of polypyrrole particles: An *in vivo* study in mice. *J. Pharm. Pharmacol.* **2007**, *59*, 311–315.
32. Kang, E.; Neoh, K.; Zhang, X.; Tan, K.; Liaw, D. Surface modification of electroactive polymer films by ozone treatment. *Surf. Interface Anal.* **1996**, *24*, 51–58.
33. Goddard, J.M.; Hotchkiss, J. Polymer surface modification for the attachment of bioactive compounds. *Progr. Polymer Sci.* **2007**, *32*, 698–725.
34. Kotanen, C.N.; Guiseppi-Elie, A. Bioactive electroconductive hydrogels yield novel biotransducers for glucose. *Macromol. Symp.* **2012**, *317–318*, 187–197.
35. Kotanen, C.N.; Tlili, C.; Guiseppi-Elie, A. Bioactive electroconductive hydrogels: The effects of electropolymerization charge density on the storage stability of an enzyme-based biosensor. *Appl. Biochem. Biotechnol.* **2012**, *166*, 878–888.
36. Guiseppi-Elie, A. Electroconductive hydrogels: Synthesis, characterization and biomedical applications. *Biomaterials* **2010**, *31*, 2701–2716.
37. Kotanen, C.N.; Moussy, F.G.; Carrara, S.; Guiseppi-Elie, A. Implantable enzyme amperometric biosensors. *Biosens. Bioelectron.* **2012**, *35*, 14–26.
38. Kotanen, C.N.; Tlili, C.; Guiseppi-Elie, A. Amperometric glucose biosensor based on electroconductive hydrogels. *Talanta* **2013**, *103*, 228–235.
39. Palmisano, F.; Rizzi, R.; Centonze, D.; Zambonin, P.G. Simultaneous monitoring of glucose and lactate by an interference and cross-talk free dual electrode amperometric biosensor based on electropolymerized thin films. *Biosens. Bioelectron.* **2000**, *15*, 531–539.
40. Guiseppi-Elie, A.; Wilson, A.M.; Tour, J.M.; Brockmann, T.W.; Zhang, P.; Allara, D.L. Specific immobilization of electropolymerized polypyrrole thin films onto interdigitated microsensor electrode arrays. *Langmuir* **1995**, *11*, 1768–1776.
41. Guiseppi-Elie, A.; Brahim, S.; Slaughter, G.; Ward, K. Design of a subcutaneous implantable biochip for monitoring of glucose and lactate. *IEEE Sens. J.* **2005**, *5*, 345–355.
42. Rahman, A.R.A.; Justin, G.; Guiseppi-Elie, A. Towards an implantable biochip for glucose and lactate monitoring using micro-disc electrode arrays (MDEAs). *Biomed. Microdevices* **2009**, *11*, 75–85.
43. Aussedat, B.; Dupire-Angel, M.; Gifford, R.; Klein, J.C.; Wilson, G.S.; Reach, G. Interstitial glucose concentration and glycemia: Implications for continuous subcutaneous glucose monitoring. *Am. J. Physiol. Endocrinol. Metabol.* **2000**, *278*, E716–E728.

44. Emr, S.A.; Yacynych, A.M. Use of polymer films in amperometric biosensors. *Electroanalysis* **2005**, *7*, 913–923.
45. Fortier, G.; Belanger, D. Characterization of the biochemical behavior of glucose oxidase entrapped in a polypyrrole film. *Biotechnol. Bioeng.* **2004**, *37*, 854–858.
46. Guiseppi-Elie, A. An implantable biochip to influence patient outcomes following trauma-induced hemorrhage. *Anal. Bioanal. Chem.* **2011**, *399*, 403–419.
47. Guiseppi-Elie, A.; Koch, L.; Finley, S.H.; Wnek, G.E. The effect of temperature on the impedimetric response of bioreceptor hosting hydrogels. *Biosens. Bioelectron.* **2011**, *26*, 2275–2280.
48. Shoemaker, S.G.; Hoffman, A.S.; Priest, J.H. Synthesis and properties of vinyl monomer/enzyme conjugates. Conjugation of L-asparaginase with N-succinimidyl acrylate. *Appl. Biochem. Biotechnol.* **1987**, *15*, 11–24.
49. Wolowacz, S.E.; Yon Hin, B.F.Y.; Lowe, C.R. Covalent electropolymerization of glucose oxidase in polypyrrole. *Anal. Chem.* **1992**, *64*, 1541–1545.
50. Ahuja, T.; Mir, I.A.; Kumar, D.; Rajesh. Biomolecular immobilization on conducting polymers for biosensing applications. *Biomaterials* **2007**, *28*, 791–805.
51. Yon-Hin, B.F.Y.; Smolander, M.; Crompton, T.; Lowe, C.R. Covalent electropolymerization of glucose oxidase in polypyrrole. Evaluation of methods of pyrrole attachment to glucose oxidase on the performance of electropolymerized glucose sensors. *Anal. Chem.* **1993**, *65*, 2067–2071.
52. Lee, J.Y.; Schmidt, C.E. Pyrrole-hyaluronic acid conjugates for decreasing cell binding to metals and conducting polymers. *Acta Biomaterialia* **2010**, *6*, 4396–4404.
53. DeVolder, R.J.; Zill, A.T.; Jeong, J.H.; Kong, H. Microfabrication of proangiogenic cell-Laden alginate-g-Pyrrole hydrogels. *Biomaterials* **2012**, *33*, 7718–7726.
54. Sung, W.J.; Bae, Y.H. A glucose oxidase electrode based on polypyrrole with polyanion/PEG/enzyme conjugate dopant. *Biosens. Bioelectron.* **2003**, *18*, 1231–1239.
55. Sung, W.J.; Bae, Y.H. Glucose oxidase, lactate oxidase, and galactose oxidase enzyme electrode based on polypyrrole with polyanion/PEG/enzyme conjugate dopant. *Sens. Actuator B Chem.* **2006**, *114*, 164–169.
56. Akhtar, P.; Too, C.; Wallace, G.G. Detection of haloacetic acids at conductive electroactive polymer-modified microelectrodes. *Anal. Chim. Acta* **1997**, *341*, 141–153.
57. Cass, A.E.; Davis, G.; Francis, G.D.; Hill, H.A.O.; Aston, W.J.; Higgins, I.J.; Plotkin, E.V.; Scott, L.D.; Turner, A.P. Ferrocene-mediated enzyme electrode for amperometric determination of glucose. *Anal. Chem.* **1984**, *56*, 667–671.
58. Sung, W.J.; Bae, Y.H. A glucose oxidase electrode based on electropolymerized conducting polymer with polyanion-enzyme conjugated dopant. *Anal. Chem.* **2000**, *72*, 2177–2181.
59. Yon-Hin, B.F.; Smolander, M.; Crompton, T.; Lowe, C.R. Covalent electropolymerization of glucose oxidase in polypyrrole. Evaluation of methods of pyrrole attachment to glucose oxidase on the performance of electropolymerized glucose sensors. *Anal. Chem.* **1993**, *65*, 2067–2071.
60. Yon-Hin, B.; Lowe, C. An investigation of 3-functionalized pyrrole-modified glucose oxidase for the covalent electropolymerization of enzyme films. *J. Electroanal. Chem.* **1994**, *374*, 167–172.

61. Xu, G.; Lv, J.; Zheng, Z.; Wu, Y. Polypyrrole (PPy) Nanowire Arrays Entrapped with Glucose Oxidase Biosensor for Glucose Detection. In Proceedings of the 7th IEEE International Conference on of Nano/Micro Engineered and Molecular Systems (NEMS), Kyoto, Japan, 5–8 March 2012; pp. 511–514.
62. Abraham, S.; Brahim, S.; Ishihara, K.; Guiseppi-Elie, A. Molecularly engineered p(HEMA)-based hydrogels for implant biochip biocompatibility. *Biomaterials* **2005**, *26*, 4767–4778.
63. Yu, B.; Long, N.; Moussy, Y.; Moussy, F. A long-term flexible minimally-invasive implantable glucose biosensor based on an epoxy-enhanced polyurethane membrane. *Biosens. Bioelectron.* **2006**, *21*, 2275–2282.
64. Tsai, Y.-C.; Li, S.-C.; Liao, S.-W. Electrodeposition of polypyrrole-multiwalled carbon nanotube-glucose oxidase nanobiocomposite film for the detection of glucose. *Biosens. Bioelectron.* **2006**, *22*, 495–500.
65. Li, J.; Lin, X. Glucose biosensor based on immobilization of glucose oxidase in poly(*o*-aminophenol) film on polypyrrole-Pt nanocomposite modified glassy carbon electrode. *Biosens. Bioelectron.* **2007**, *22*, 2898–2905.
66. Kong, T.; Chen, Y.; Ye, Y.; Zhang, K.; Wang, Z.; Wang, X. An amperometric glucose biosensor based on the immobilization of glucose oxidase on the ZnO nanotubes. *Sens. Actuator B Chem.* **2009**, *138*, 344–350.
67. German, N.; Ramanavicius, A.; Voronovic, J.; Ramanaviciene, A. Glucose biosensor based on glucose oxidase and gold nanoparticles of different sizes covered by polypyrrole layer. *Colloid Surface Physicochem. Eng. Aspect* **2012**, *413*, 224–230.
68. Wang, J.; Musameh, M. Carbon-nanotubes doped polypyrrole glucose biosensor. *Anal. Chim. Acta* **2005**, *539*, 209–213.
69. Demoustier-Champagne, S.; Ferain, E.; Jérôme, C.; Jérôme, R.; Legras, R. Electrochemically synthesized polypyrrole nanotubules: effects of different experimental conditions. *Eur. Polymer J.* **1998**, *34*, 1767–1774.
70. Chen, X.; Issi, J.P.; Devaux, J.; Billaud, D. Chemically oxidized polypyrrole: Influence of the experimental conditions on its electrical conductivity and morphology. *Polymer Eng. Sci.* **1995**, *35*, 642–647.
71. Levy, B. Lactic acidosis and hyperlactatemia. In *Yearbook of Intensive Care and Emergency Medicine*; Vincent, J.-L., Ed.; Springer: Berlin/Heidelberg, Germany, 2006; Volume 2006, pp. 88–98.
72. Callaway, D.W.; Shapiro, N.I.; Donnino, M.W.; Baker, C.; Rosen, C.L. Serum lactate and base deficit as predictors of mortality in normotensive elderly blunt trauma patients. *J. Trauma* **2009**, *66*, 1040–1044.
73. Wisniewski, N.; Reichert, M. Methods for reducing biosensor membrane biofouling. *Colloid Surface B Biointerface* **2000**, *18*, 197–219.
74. Wilson, G.S.; Gifford, R. Biosensors for real-time *in vivo* measurements. *Biosens. Bioelectron.* **2005**, *20*, 2388–2403.
75. Rigby, G.; Ahmed, S.; Horseman, G.; Vadgama, P. *In vivo* glucose monitoring with open microflow-influences of fluid composition and preliminary evaluation in man. *Anal. Chim. Acta* **1999**, *385*, 23–32.

76. Valdes, T.; Moussy, F. *In vitro* and *in vivo* degradation of glucose oxidase enzyme used for an implantable glucose biosensor. *Diabetes Tech. Therapeut.* **2000**, *2*, 367–376.
77. Kulcu, E.; Tamada, J.A.; Reach, G.; Potts, R.O.; Lesho, M.J. Physiological differences between interstitial glucose and blood glucose measured in human subjects. *Diabetes Care* **2003**, *26*, 2405–2409.
78. Schmidtke, D.W.; Freeland, A.C.; Heller, A.; Bonnecaze, R.T. Measurement and modeling of the transient difference between blood and subcutaneous glucose concentrations in the rat after injection of insulin. *PNAS* **1998**, *95*, 294–299.
79. Koschwanez, H.E.; Reichert, W.M. *In vitro*, *in vivo* and post explantation testing of glucose-detecting biosensors: Current methods and recommendations. *Biomaterials* **2007**, *28*, 3687–3703.
80. Updike, S.J.; Shults, M.C.; Rhodes, R.K.; Gilligan, B.J.; Luebow, J.O.; von Heimburg, D. Enzymatic glucose sensors: Improved long-term performance *in vitro* and *in vivo*. *ASAIO J.* **1994**, *40*, 157–163.
81. Armour, J.C.; Lucisano, J.Y.; McKean, B.D.; Gough, D.A. Application of chronic intravascular blood glucose sensor in dogs. *Diabetes* **1990**, *39*, 1519–1526.
82. Youssef, J.E.; Castle, J.R.; Engle, J.M.; Massoud, R.G.; Ward, W.K. Continuous glucose monitoring in subjects with type 1 diabetes: Improvement in accuracy by correcting for background current. *Diabetes Tech. Therapeut.* **2010**, *12*, 921–928.
83. Jeong, R.-A.; Hwang, J.Y.; Joo, S.; Chung, T.D.; Park, S.; Kang, S.K.; Lee, W.-Y.; Kim, H.C. *In vivo* calibration of the subcutaneous amperometric glucose sensors using a non-enzyme electrode. *Biosens. Bioelectron.* **2003**, *19*, 313–319.